Synergistic Effects of Tetrabutyl Titanate on Intumescent Flame-Retarded Polypropylene

Anna Zheng, Yin Xia, Na Li, Zongwen Mao, Yong Guan

Shanghai Key Laboratory of Advanced Polymeric Materials, Key Laboratory for Ultrafine Materials of Ministry of Education, School of Materials Science and Engineering, East China University of Science and Technology, Shanghai 200237, China
Correspondence to: Y. Guan (E-mail: yguan@ecust.edu.cn) and A. Zheng (E-mail: zan@ecust.edu.cn)

ABSTRACT: The synergistic mechanism of tetrabutyl titanate (TBT) in the intumescent flame-retardant polypropylene (PP) composites was investigated in this work. The intumescent flame-retardant was composed of pentaerythritol (PER) as a carbonizing agent ammonium polyphosphate (APP) as a dehydrating agent and blowing agent. Five different concentrations (1, 1.25, 1.5, 1.75, 2 wt %) of TBT were incorporated into flame retardant formulation to investigate the synergistic mechanism. The thermal degradation and flammability of composites were characterized by thermogravimetric analysis (TGA), limiting oxygen index (LOI), and UL-94 tests. The morphology and chemical structure of char layer was characterized by scanning electron microscopy (SEM), Fourier transform infrared spectroscopy (FTIR), and energy dispersive spectrometer (EDS). The results showed that LOI was increased from 27.8 to 32.5%, with the increase of TBT content from 0 to 1.5 wt %. Results from SEM, and FTIR demonstrated that TBT could react with APP and PER to form the stable char layer. © 2013 Wiley Periodicals, Inc. J. Appl. Polym. Sci. 130: 4255–4263, 2013

INTRODUCTION

PP has been extensively applied in many fields, such as apparel, upholstery, floor coverings, hygiene medical, car industry, automobile industry, textiles, etc.,[1] because of its easy processing property, low density, excellent mechanical properties.[2–4] However, its inflammability limits its applications in many fields such as electronic appliances where high flame retardancy is required. In the past decades, intumescent flame retardants (IFRs) have attracted the attention of the researches, which have been confirmed to be effective for PP. When the content of IFR reaches 25–30 wt %, the LOI of PP can be increased to more than 28%, and UL-94 test can achieve V-0.[5–9]

IFRs systems are comprised of a dehydrating agent, a carbonizing agent, and a blowing agent. For example, a classic IFR system in flame-retarded PP is composed of APP, PER.[10] In this system, APP acts as a dehydating and blowing agent, PER acts as a carbonizing agent. The mechanism is believed that IFR can form the char layer to block heat and mass transfer between the gas and the condensed phases.[11] The char layer is formed by the esterification and cross-linking reactions of the flame retardant and polymer matrix.[12]

Flame retardancy synergists also play an important role in PP/IFR systems. To achieve good flame retardancy, the inorganic fillers such as zeolites,[13] organ-montmorillonite,[14] calcium carbonate ($CaCO_3$), talc,[15] and organoboron siloxane[16,17] have been introduced into IFRs. For metallic oxide, Fe_2O_3,[18] Al_2O_3,[19] Sb_2O_3,[20] MnO_2[21,22] have been investigated in the PP/IFR system. However, it hasn't been reported the reaction mechanism of esterification catalyst in the PP/IFR systems.

In this work, tetrabutyl titanate (TBT) was introduced to the PP/IFR composites to improve the flame retardant performance of PP/IFR, and the synergistic mechanism of which was discussed in detail. The morphology of the char layers, the flame retardant properties of the systems and the decomposition of PP, PP/IFR, and PP/IFR/TBT systems were investigated by LOI, UL-94, FTIR, TGA, SEM, and EDS.

MATERIALS AND EXPERIMENTAL

Materials

PP resin (homopolymer, melt flow index: 2.8 g/10 min) used in this work was supplied by Zhenhai Petroleum, China. APP ($n > 1000$, Crystalline form II) of average particle size of 10 μm was supplied by Shanghai Xusen Non-Halogen Smoke Suppressing Fire Retardants, China. PER (CP) was produced by Shanghai Lingfeng Chemical, China. TBT (AR) was offered by Shanghai Lingfeng Chemical, China. Antioxidant B215 was supplied by Suzhou Jixin Company. All the chemicals were used as received.

Table I. LOI and UL-94 Results of PP/IFR Composites with Different Ratio of APP/PER

m(PP)/g	m(APP)/g	m(PER)/g	Ratio of APP/PER (m/m)	LOI (%)	UL-94
36	12	0	1 : 0	18.9 ± 0.2	No rating
36	6	6	1 : 1	26.3 ± 0.2	V-1
36	7.2	4.8	1.5 : 1	27.8 ± 0.3	V-0
36	8	4	2 : 1	26.9 ± 0.2	V-1
36	9	3	3 : 1	26.2 ± 0.1	V-2
36	9.6	2.4	4 : 1	25.5 ± 0.2	V-2

Sample Preparation

Intumescent flame retardants (IFRs) consisted of APP, PER, and TBT. The ratio of APP to PER was set at 1.5 : 1, and the dosage of TBT varied from 0 to 2 wt %. Intumescent flame retardant PP composites (IFR-PP) were prepared by blending PP powder, IFR, antioxidant B215 and TBT using an internal mixer (Su70-1, SuYan Technology Company, China), at 180°C and the rotate speed of 80 r min^{-1}. Then the mixed materials were pressed into sheets by compression molding (XQLB-350*350, Shanghai First Rubber Machinery Factory, China) at 180°C. The composite sheets were further cut into standard specimens for mechanical properties and flame retardancy measurements.

Flame Retardancy Tests

The flame retardancy of all samples was characterized by LOI and UL-94 methods. LOI data of all samples were recorded at room temperature on an Oxygen Index Instrument (JF-3) produced by Jiangning Nanjing Analytical Instrument Factory, China, according to ISO 1210:1992 Standard. The dimensions of all samples were 130 × 6.5 × 3 mm^3. Vertical burning ratings of all samples were measured on a Vertical Burning Tester (CZF-2) produced by Jiangning Nanjing Analytical Instrument Factory, China, with sample dimensions of 125 × 12.5 × 3.0 mm^3, according to ISO 1210:1992 Standard.

Thermogravimetric Analysis Test

Thermogravimetric analysis was carried out by a NETZSCH STA 409 thermal analyzer at a heating rate of 10 C min^{-1} under nitrogen atmosphere. The temperature was from ambient to 600°C. The weight of each sample was around 10 mg.

Scanning Electron Microscopy

SEM (JSM-6360 Scanning Electron Microscopy) was used to examine the morphology of the char layer. The char layer was obtained from muffle furnace at 400°C for 30 min. The accelerating voltage was 15 kV. The surface of char layer was sputter-coated with gold layer prior to measurement.

Fourier Transform Infrared Spectroscopy

The FTIR spectra were recorded by a NICOLET 5700 spectrometer. The char layer of the PP/IFR composites, obtained after the treatment in the muffle furnace at 400 and 600°C, respectively, were mixed with KBr powders for FTIR measurement.

Mechanical Properties

The tensile strength and flexural strength of the PP/IFR composites were evaluated by a CMT-4204 machine at 20°C. The dimensions of the flexural samples were as follows: 80 × 10 × 4 mm^3, according to ISO 178:1993. The tensile strength tests were carried out according to ISO 1184-1983.

The impact strength was measured by a JJ-20 Impact Machine according to ISO 180:1993.

Strength of the Residual Charred Layer

The strength of the char layer obtained from LOI tests was examined by HY-0230 machine. The char layer was placed on a circular flat and suffered a pressure, and then the load was recorded when the char layer was broken.

Energy Dispersive Spectrometer

The elements of the char layers were tested by EDS (Falcon Energy Dispersive Spectrometer). The char layer was obtained from muffle furance at 400°C for 30 min. The surface of char layer was sputter-coated with gold layer prior to measurement.

Cone Calorimeter Analysis

Cone Calorimeter tests were performed by using a Stanton Redcroft Cone Calorimeter following the procedure defined in ASTM E 1354. The samples were put in horizontal orientation at an incident flux of 35 kW m^{-2}. Sample size was 100 mm × 100 mm × 4 mm. The results were the average values from three tests.

RESULTS AND DISCUSSION

LOI and UL-94 Analysis

Table I shows the LOI values and the UL-94 tests of the PP/IFR systems with different ratio of APP/PER. Obviously, with the increasing addition of APP, the LOI value firstly increased, then decreased, and reached the maximum value at around 27.8, when the ratio of APP/PER was 1.5 : 1 (wt/wt). At the same time, the UL-94 rating could reach V-0. Because the reaction between APP and PER can generate the charred layer which can isolate the oxygen and heat. When the content of APP is low, the charred layer is crumbly which is useless in holding back the oxygen and heat. On the other hand, when the content of APP reached high enough, the reaction would produce plenty of gas which made the stable charred layer broken. Therefore, there is an optimal ratio of APP/PER 1.5 : 1 (wt/wt) for the APP/PER systems.

Table II listed that the LOI and UL-94 results of PP/IFR/TBT composites with the different ratio of TBT. Comparing Sample 1$^\#$ and 6$^\#$, 3.2% of increase in LOI could be observed with an increase in the TBT content from 0 to 2 wt %. It confirmed

Table II. LOI and UL-94 Results of PP/IFR/TBT Composites

Sample	m(PP)/g	m(APP)/g	m(PER)/g	m(TBT)/g	LOI	UL-94
0#	100.00	0.00	0.00	0.00	18.0 ± 0.2	No rating
1#	75.00	15.00	10.00	0.00	27.8 ± 0.2	V-0
2#	74.00	15.00	10.00	1.00	30.5 ± 0.3	V-0
3#	73.75	15.00	10.00	1.25	32.0 ± 0.2	V-0
4#	73.50	15.00	10.00	1.50	32.5 ± 0.4	V-0
5#	73.25	15.00	10.00	1.75	31.8 ± 0.3	V-0
6#	73.00	15.00	10.00	2.00	31.0 ± 0.2	V-0
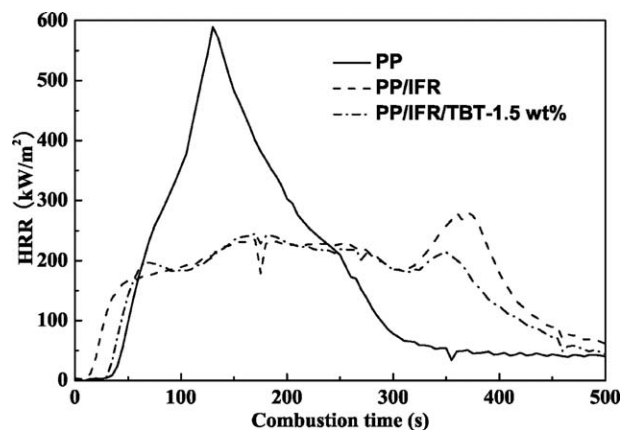
Figure 1. HRR curves of PP, PP/IFR, and PP/IFR/TBT-1.5 wt %.

that the synergistic effect of TBT could give the excellent flame-retardancy of PP/IFR systems.

The results of LOI indicated that the introduction of IFR could significantly improve the flame-retardant property of PP system. The LOI increased from 18.0 to 27.8%. When the content of APP/PER was over 25 wt %, the UL-94 rate reached V-0 as shown in Table II. TBT could catalyze the esterification reaction of APP/PER, the flame-retardant property of the PP/IFR system could be further improved in the presence of TBT. With the increase of TBT content, LOI increased first and then decreased. Initially, with the increase of TBT from 0 to 1.5 wt %, the LOI
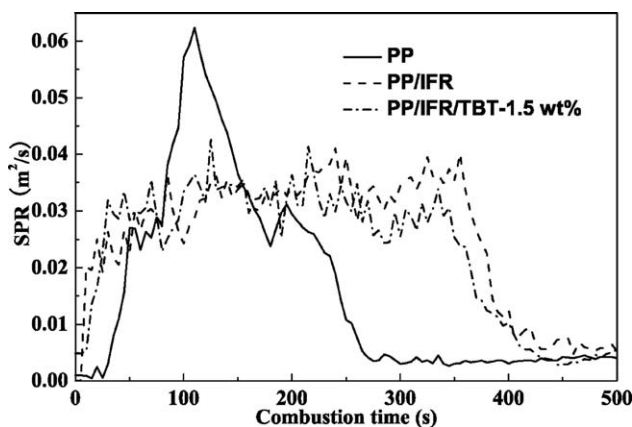
could be improved from 27.8 to 32.5%. Subsequently, the LOI values of the PP/IFR systems decreased from 32.5 to 31.0%, TBT content was beyond 1.5 wt %. The LOI test demonstrated that 1.5 wt % was the optimal addition of TBT for the PP/IFR systems to achieve the excellent flame-retardant property. The reason might be that TBT could react with APP, and also react with PER to produce more cross-linking points. With the increase of TBT, the crosslinking density of the char layer was increased, which made the char layer more compact to shield the heat and oxygen. On the other hand, with the increase of TBT, the reactive groups also increased, which could decrease
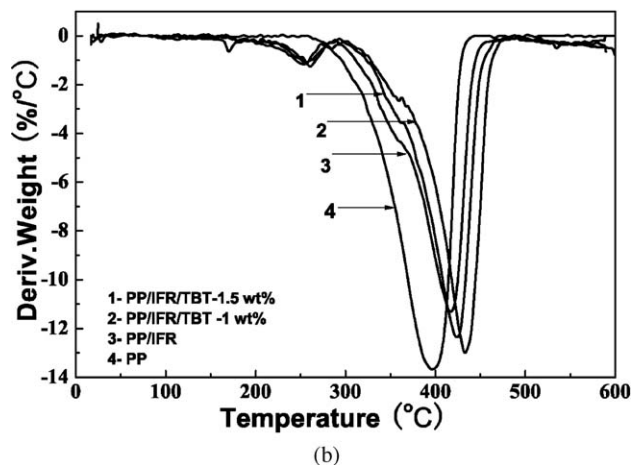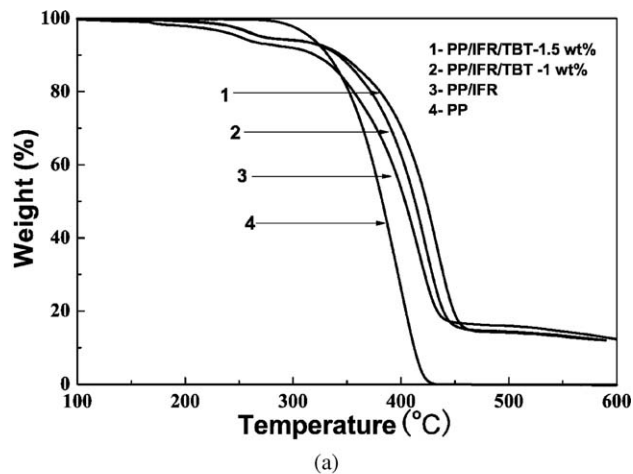

(a)

(b)

Figure 3. Thermogravimetric behavior of composite samples under nitrogen atmosphere.

Figure 2. Rate of smoke production (SPR) curves of PP, PP/IFR, and PP/IFR/TBT-1.5 wt %.
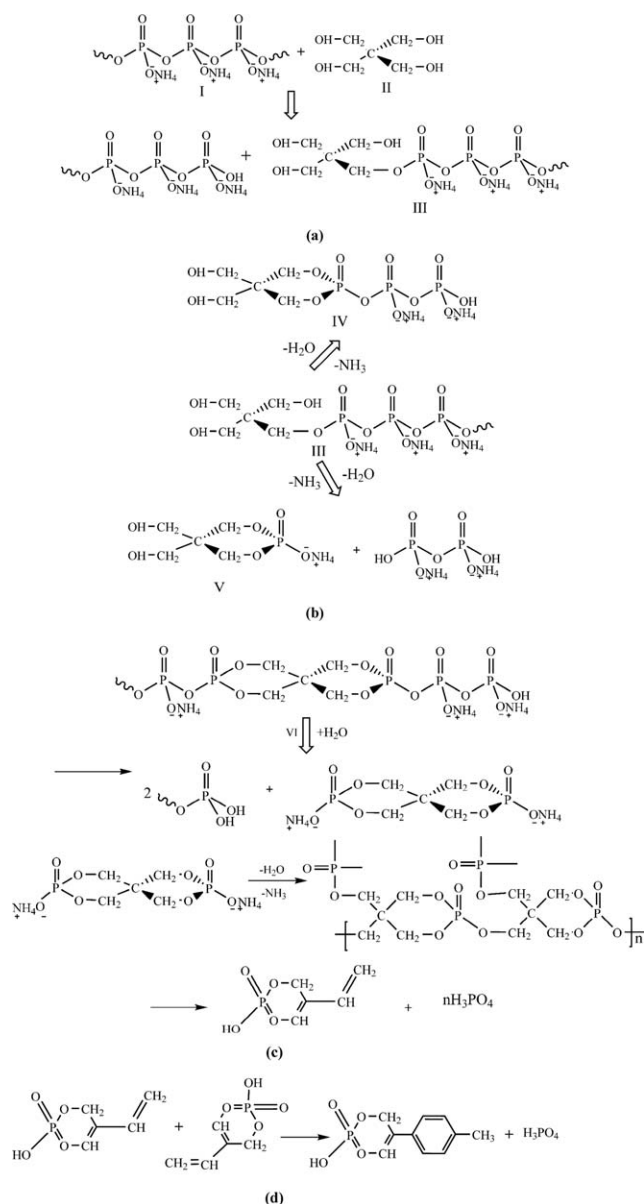
Figure 4. Decomposition mechanism of the PP/IFR.

the crosslinking density. Therefore, 1.5 wt % was the balance point of the TBT content between crosslinking points and reactive groups.

The results of UL-94 were shown in Table II confirmed that all the samples except sample $0^{\#}$ could reach V-0.

Cone Calorimeter Analysis

The heat release rate (HRR) was regarded as the most important parameter for measuring the development and spreading of fire. Figure 1 showed the HRR curves of PP, PP/IFR, and PP/IFR/TBT-1.5 wt %. It indicated that the PHRR (peak of HRR) of PP/IFR/TBT-1.5 wt % (214.0 KW m^{-2}) was the smallest compared with that of PP/IFR (280.0 KW m^{-2}) and PP (589.2 KW m^{-2}).

Rate of smoke production (SPR) curves of PP, PP/IFR, and PP/IFR/TBT-1.5 wt % during the whole combustion process were

presented in Figure 2. The order of the SPR peak values was PP/IFR/TBT (0.039 m^2 s^{-1}) < PP/IFR (0.043 m^2 s^{-1}) < PP (0.062 m^2 s^{-1}). These results suggested that the SPR decreased significantly when TBT was introduced into the PP/IFR system.

Thermogravimetric Analysis and Mechanism of Synergism

Figure 3 showed the thermogravimetric behavior of composite samples under nitrogen atmosphere. Comparing the TGA curve of PP/IFR with that of PP, it was found that IFRs effectively improved the flame retardant property of PP. PP decomposed initially at about 347.1°C, the T_{max} value occured at 394.6°C. There was no residue above 450°C. The decomposition mechanism of the PP/IFR was schematically shown in Figure 4. It included three steps. The first step initially at about 231.2°C due to the decomposition of APP (I), the alcoholysis reaction of PER (II) to form the products with phosphaester-bond (III). The second step [Figure 4(c)] occured at 369.7°C which was the main decomposition process, releasing water and ammonia and forming the stable cyclic ester. The T_{max} value for this step was 416.7°C and the mass loss was 77.04% in this step. The third step occurred at 434.2°C, which was the pyrogenation process of ester[23,24] [Figure 4(d)].
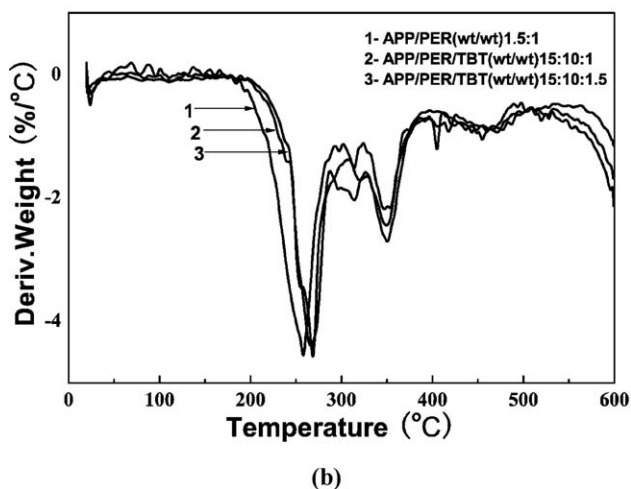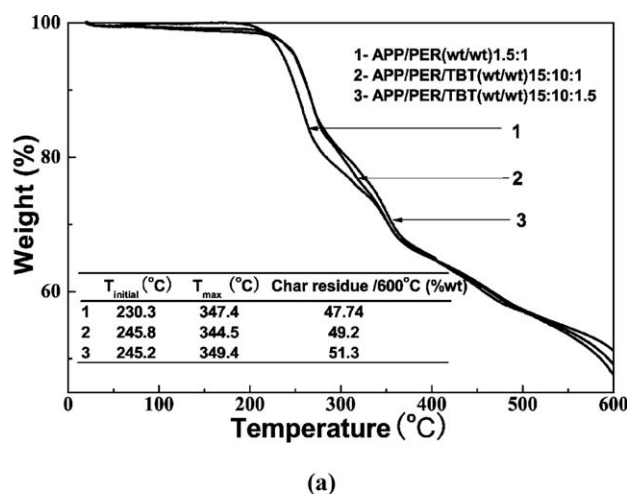

(a)

(b)

Figure 5. Thermal behavior of different ratio of APP/PER/TBT under nitrogen atmosphere.
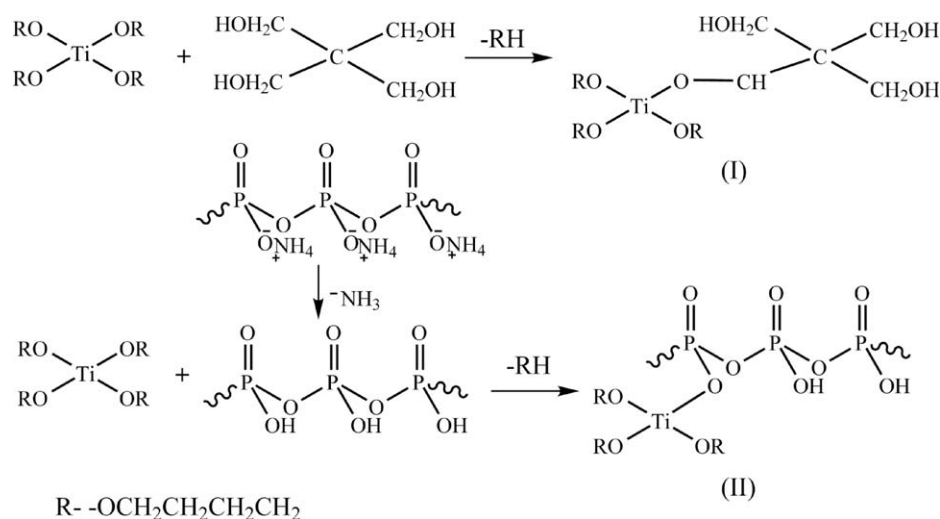
Figure 6. Reaction of TBT with APP and PER.

When TBT was introduced into the PP/IFR system, it could effect the maximum decomposition temperature of APP and PER which increased from 416.7 to 431.2°C, when TBT content was 1 wt %. However, the content of TBT reached 1.5 wt %, the

Figure 7. FTIR spectra of PP, PP/IFR, PP/IFR/TBT- 1 wt % and PP/IFR/TBT- 1.5 wt %.

maximum decomposition temperature was lower than that of PP/IFR/TBT-1 wt % system. The effect of TBT content on the thermostability is shown in Table III. It might be the reactive groups of PP/IFR/TBT-1.5 wt % were more than that of PP/IFR/TBT-1 wt %, which lowered the maximum decomposition temperature.
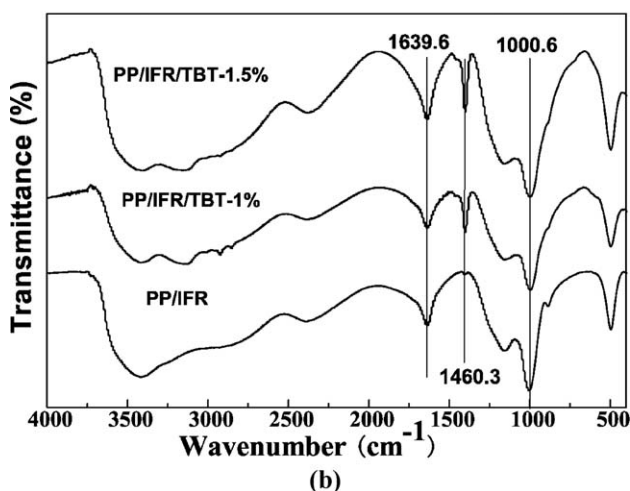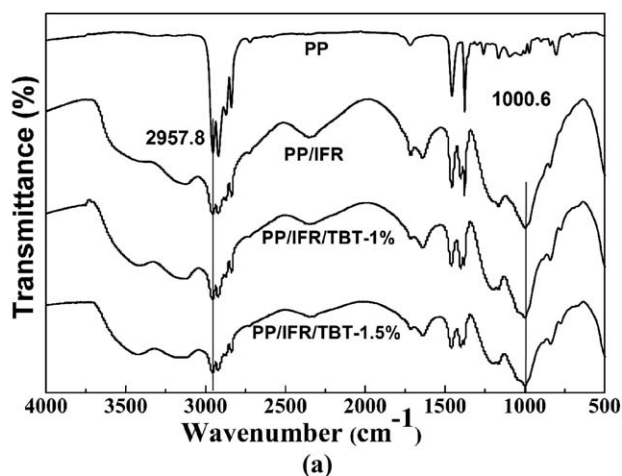
Mechanism of Synergism

Figure 5 showed the thermal behavior of different ratio of APP/PER/TBT under nitrogen atmosphere. There were three steps in the decomposition of APP/PER. First, the esterification reaction between APP and PER began at 230.3°C, and ended at 270.7°C. The second step happened between 341.2 and 362.3°C which was the important step to form the char layer. The major release of the ammonia and water happened in this step. The third step occurred at 432.6°C, which was the pyrogenation process of ester.[23,24] The char residue of the APP/PER at the weight ratio of 1.5 : 1 was 47.74 wt % at 600°C.

TBT had a great influence on the reaction between APP and PER, especially on the char residue. When the weight ratio of APP/PER/TBT was 15 : 10 : 1, the first step occurred at 245.8°C which was higher than that of APP/PER system. With the increase of the TBT content, the initial decomposition temperature showed little change. However, the char residue was increased, with the increase of TBT content. When the weight ratio of APP/PER/TBT was 15 : 10 : 1.5, the char residue was

Table III. TGA and the Char Residue Data of the PP, PP/IFR with and Without TBT

Samples	$T_{initial}$(°C)	T_{max} (°C)	Char residue/ 600°C (wt %)
PP	347.1	394.6	0.00
PP/IFR	231.2	416.7	12.34
PP/IFR/TBT-1 wt %	239.4	431.2	12.09
PP/IFR/ TBT-1.5 wt %	233.6	427.7	11.98

Table IV. Assignments of FT-IR Absorption Peaks

Wavenumber (cm^{-1})	Assignment	References
1000.6	v_{sym} of PO$_3$ in phosphate-carbon complex	27
1088	v_{sym} of P—O in P—O—P	27,28
1460.3	—CH$_2$	27
1639.6	the strength mode of P—OH (Ar)	29
2850	v_{sym} of C—H in CH$_2$ or CH$_3$	27,30
2920	v_{as} of C—H in CH$_2$ or CH$_3$	27

Figure 8. EDS spectra of PP, PP/IFR, PP/IFR/TBT- 1wt % and PP/IFR/TBT- 1.5 wt %.

increased to 51.30 wt %. It was probably that TBT could react with APP and PER[25,26] (Figure 6), which produced more cross-linking points to form cross-linking structure. Therefore, the char layer was more stable to block the transfer of heat and oxygen.

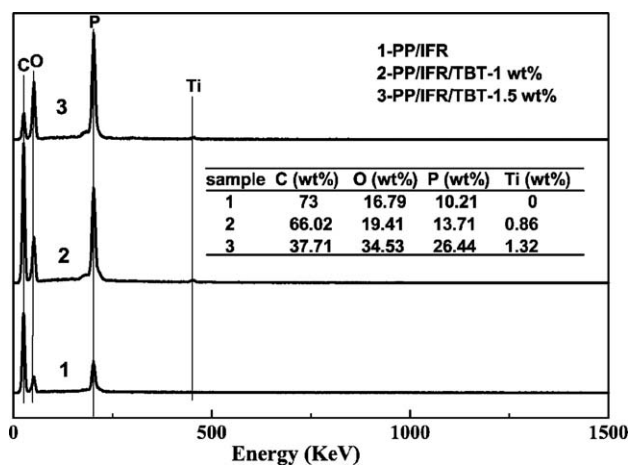**Chemical Structure Analysis of the Char Layer**

The structure and formation of the char layer are the vital factors to the final fire-resistance property. Therefore, further investigation was conducted on the chemical structure of the char layer to understand the synergistic effect in this work.

Figure 7 showed the FTIR curves of PP, PP/IFR, PP/IFR/TBT-1 wt % and PP/IFR/TBT- 1.5 wt % heated in the muffle at 300°C (a) and 400°C (b), respectively. The detailed assignments of FTIR spectra in Figure 7 and the corresponding references were presented in Table IV.

Two regions had changed when TBT was introduced into the PP/IFR system. The decomposition of PP began at 347°C, then the peak at 1458.0 cm^{-1} correspond to the CH$_2$ or CH$_3$ deformation vibration of PP was set as the base peak.

The peak of 1000.6 cm^{-1} is attributed to the PO$_3$ asymmetric vibration in the phosphate-carbon complex. Compared with intensity of the base peak, the intensity of this peak was PP/IFR < PP/IFR/TBT-1 wt % < PP/IFR/TBT-1.5 wt %, which indicated that the content of P increased in the crosslinking structure and TBT catalyzed the esterification reaction of IFR.

The peak at 1639.6 cm^{-1} is assigned to the vibration of P-OH. Compared with intensity of the base peak, the peaks of the P—OH groups in the intumescent carbonaceous char structure

of the PP/IFR/TBT system were higher and broader than those of the PP/IFR, indicating TBT, as a catalyst, had a synergistic effect on the formation of char layers containing P—OH structure. It had the same conclusion from Figure 7(b). Results of the FTIR confirmed that TBT added to the PP/IFR system, could form the crosslinking structures.

The EDS spectra in Figure 8 showed the element composition of the char layer of the PP/IFR and PP/IFR/TBT systems. With the increase of the TBT content, the content of C was decreased from 73 to 37.71 wt %, while P content was increased from 10.21 to 26.44 wt %. It confirmed that TBT could catalyze the reaction of IFR to form the crosslinking structure mainly containing PO$_3$ group. The result of EDS was the same as that of FTIR. Therefore, TBT could also react with APP and PER, the crosslinking structure contained Ti. Because of the reaction of TBT/APP and TBT/PER, the char layer was more compact to block the transfer of heat and oxygen.

Strength of the Char Layer

During heating, the gas was produced which could swell the char layer to form the cellular char layer. If the char layer had the low intensity, it would be broken easily, which could not block the diffusion of heat and mass between the gas and condensed phases. Consequently, the intensity of the char layer was
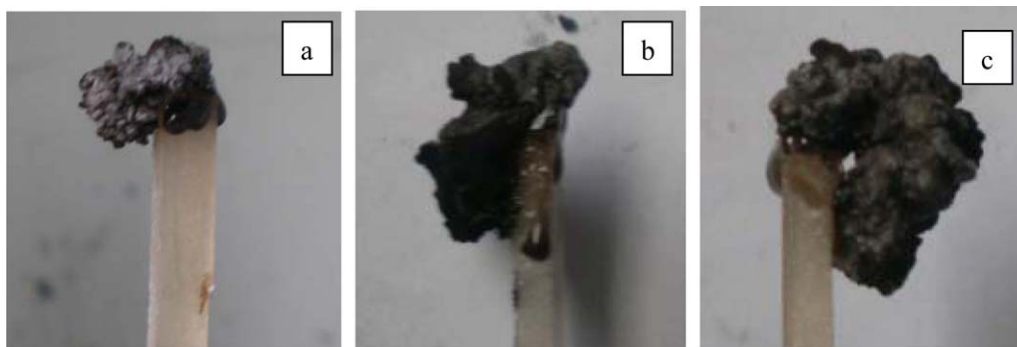
Figure 9. Photographs of the samples after LOI tests. [Color figure can be viewed in the online issue, which is available at wileyonlinelibrary.com.]
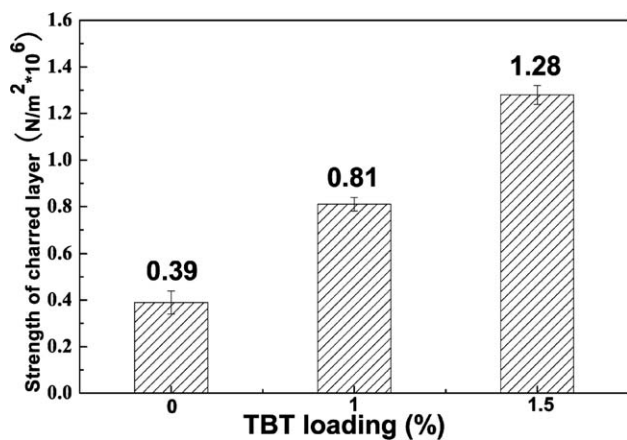
Figure 10. Strength of the char layers with different content of TBT.

the important factor for final fire-resistance of the flame retardant polymer materials.

Figure 9 showed the photographs of the samples after LOI tests. The char layer of PP/IFR was smaller than that of PP/IFR/TBT. With the increase of the TBT content, the content of the char layer also increased. When the TBT content reached 1.5 wt %, it left more char residue on the surface of the sample to protect the underlying materials.

To confirm the above explanation, the strength test of the char layers with different content of TBT were conducted by compressing the char layer till its breakage with a universal test machine. The results were shown in Figure 10. The strength of the char layer without TBT was 0.39×10^6 N m^{-2}, when the 1 wt % TBT was introduced in the system, the strength of the char layer increased to 0.81×10^6 N m^{-2}. With the increase of the TBT content, it increased from 0.81×10^6 to 1.28×10^6 N m^{-2}. It indicated that TBT could easily react with APP and PER to form the crosslinking structure to improve the strength of the char layer.
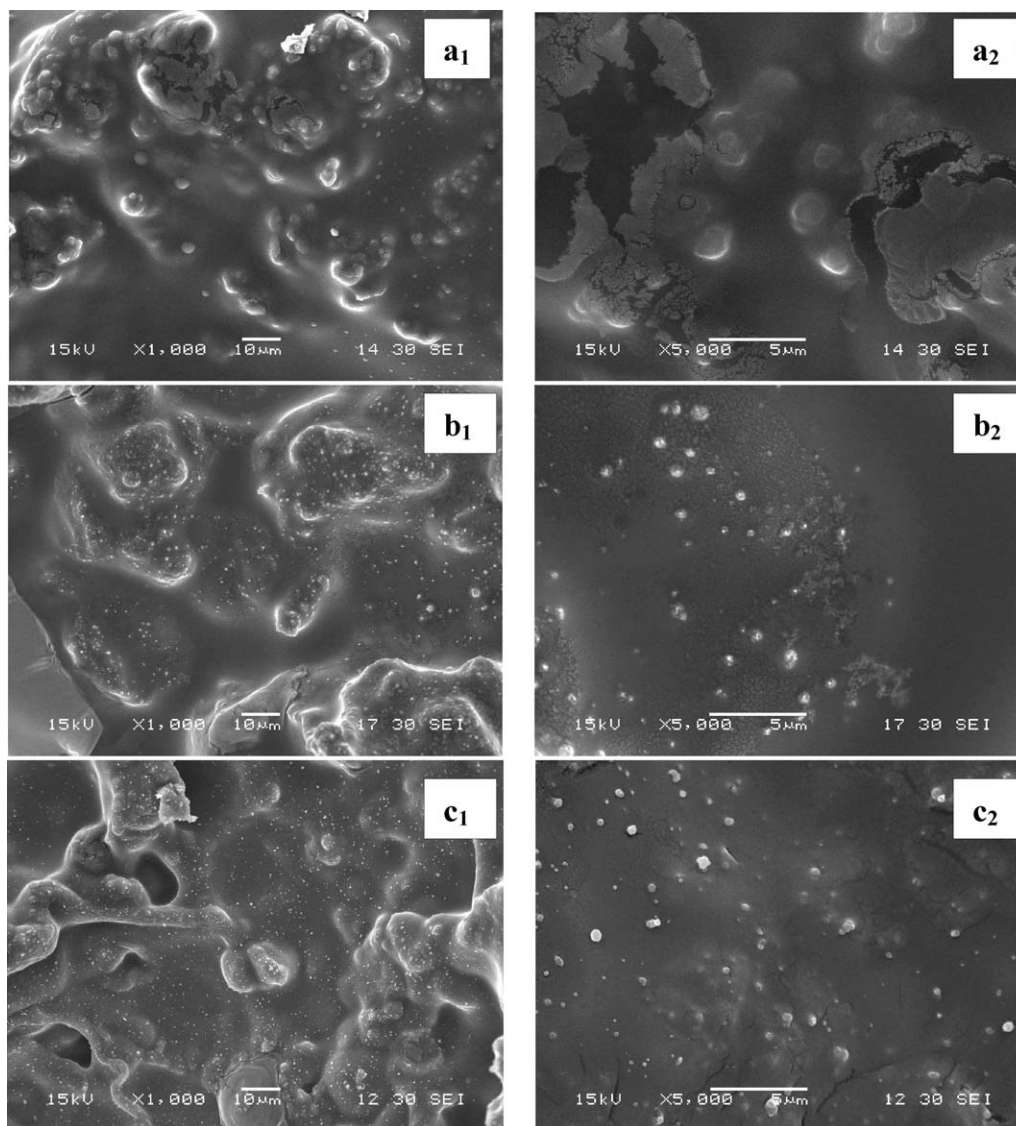

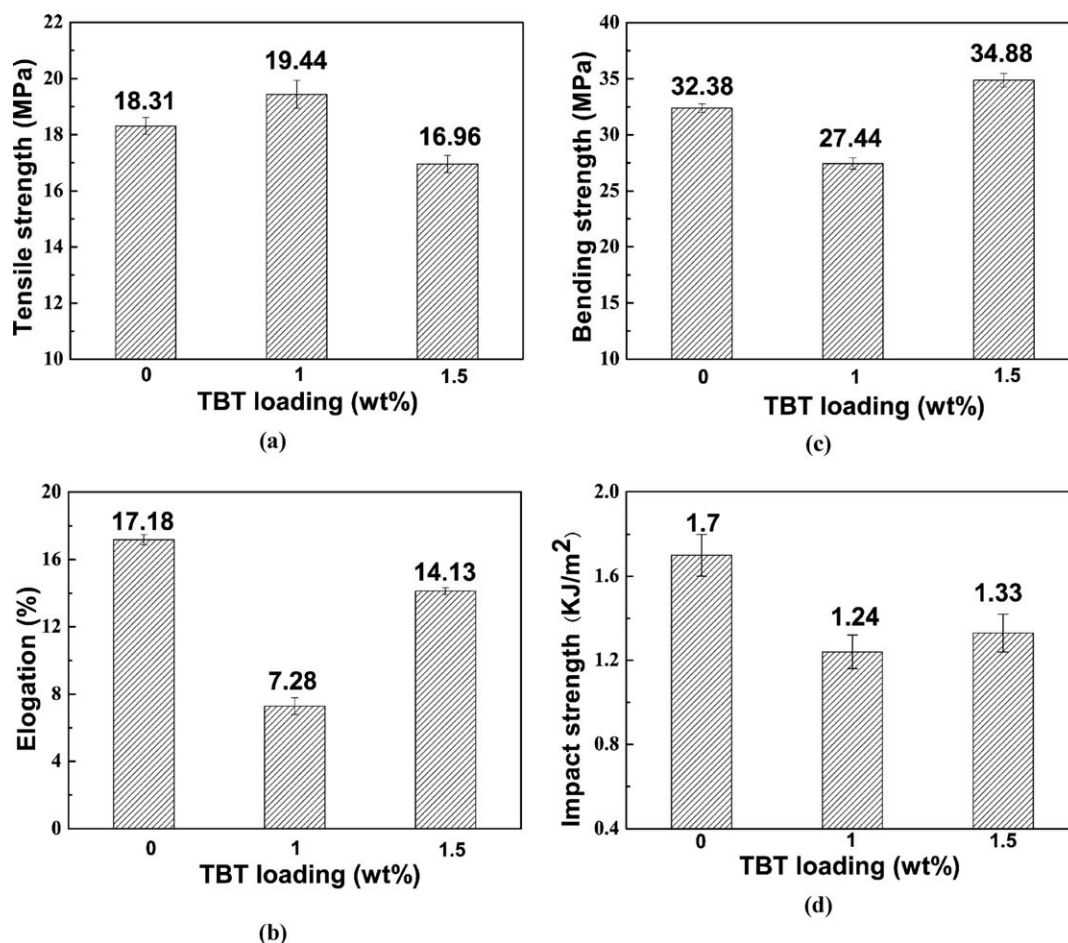**Figure 11.** SEM images of the char layers of samples.

Figure 12. Mechanical properties of PP/IFR and PP/IFR/TBT systems.

Morphology of the Char Layer

The morphology of the char layer is the most important factor to the flame retardant property. The smoother the char layer is, the stronger the flame retardant will be.

The morphology of the char layers of samples were examined by SEM, as shown in Figure 11. The char layers were prepared by heated in the muffle furance at 400°C for 30 min. There were some cracks and holes in the microstructures of the char layer of the PP/IFR blends [Figure 11(a_1,a_2)], which led to form the fragile and loose char layer. Therefore, during burning, heat and flammable volatiles could easily penetrate the char layer into the flame zone. Compared with PP/IFR system, the surfaces of the char layers of PP/IFR/TBT were more compact and smoother as shown in Figure 11(b,c). For the TBT systems, the surface of the char layer of PP/IFR/TBT-1.5 wt % [Figure 11(c_1,c_2)] was more compact and had less cracks and holes than that of PP/IFR/TBT-1 wt % [Figure 11(b_1,b_2)]. It was probably that TBT could react with APP and PER to form the stably crosslinking char layers. The optimal loading of TBT in the PP/IFR system was 1.5 wt %, in consistent with the LOI results.

Mechanical Properties of the PP/APP/PER and PP/APP/PER/TBT Blends

As shown in Figure 12 the mechanical properties of PP/IFR and PP/IFR/TBT systems. When the TBT was introduced into the

PP/IFR system, the elongation and the impact strength was decreased, because of poor compatibility. The poor compatibility blocked the molecular motion. For the tensile strength, when the content of TBT was 1 wt %, the tensile strength was increased to 19.44 MPa. With the increase of TBT content, the tensile strength decreased. But for the bending strength, with the increase of TBT content, the bending strength had a little increased. IFR had the significant effect on the mechanical property of PP/IFR system, because of high addition. Therefore, in order to improve the compatibility of PP composites system, the compatibility between IFR and PP should be improved.

CONCLUSIONS

A synergistic effect on flame retardancy was observed when TBT was introduced into PP/IFR system. The results of LOI and UL-94 burning tests indicated that TBT had a significant effect on flame retardancy. When the content of TBT reached 1.5 wt %, the LOI of the composites was increased to 32.5%, and reached the UL-94 V-0 rating. TGA results showed that when TBT content was 1.5% the maximum decomposition temperature of APP and PER increased from 416.7 to 427.7°C. The SEM images, together with the strength of char layers and TGA data, indicated that TBT could react with APP and PER which would produce more crosslinking points to form smoother, more stable and compact char layers. Therefore, the addition of TBT

could effectively block heat and oxygen transfer to protect the matrix. All the results confirm that TBT is an effective synergistic agent in the halogen-free flame-retardant system.

ACKNOWLEDGMENTS

REFERENCES

1. Zhang, S.; Richard, H. A. *Prog. Polym. Sci.* **2003**, *28*, 1517.

2. Song, P. G.; Shen, Y.; Du, B. X.; Peng, M.; Shen, L.; Fang, Z. P. *Appl. Mater. Inter.* **2009**, *1*, 452.

3. Uotila, R.; Hippi, U.; Paavola, S.; Seppālā, *J. Polymer* **2005**, *46*, 7923.

4. Li, Q.; Jiang, P. K.; Su, Z. P.; Wei, P.; Wang, G. L.; Tang, X. Z. *J. Appl. Polym. Sci.* **2005**, *96*, 854.

5. Wu, Q.; Qu, B. *J. Polym. Degrad. Stabil.* **2001**, *74*, 255.

6. Lv, P.; Wang, Z. Z.; Hu, K. L.; Fan, W. C. *Polym. Degrad. Stabil.* **2005**, *90*, 523.

7. Li, B.; Xu, M. *J. Polym. Degrad. Stabil.* **2006**, *91*, 1380.

8. Chen, Y. H.; Wang, Q. *Polym. Degrad. Stabil.* **2007**, *92*, 280.

9. Tang, Y.; Hu, Y.; Song, L.; Zong, R. W.; Gui, Z.; Fan, W. C. *Polym. Degrad. Stabil.* **2006**, *91*, 234.

10. Chiu, S. H.; Wang, W. K. *Polymer* **1998**, *39*, 1951.

11. Bourbigot, S.; Le, B. M.; Delobel, R. *Faraday Trans.* **1996**, *92*, 149.

12. Demir, H.; Arkìs, E.; Balköse, D.; Ülkü, S. *Polym. Degrad. Stabil.* **2005**, *89*, 478.

13. Bourbigot, S.; Le, B. M.; Delobel, R.; Brĕant, P.; Tremillon, J. M. *Polym. Degrad. Stabil.* **1996**, *54*, 275.

14. Almeras, X.; Le, B. M.; Hornsby, P.; Bourbigot, S.; Marosi, G.; Keszei, S.; Poutch, F. *Polym. Degrad. Stabil.* **2003**, *82*, 325.

15. Ravadits, I.; Toth, A.; Marosi, G.; Márton, A.; Szép, A. *Polym. Degrad. Stabil.* **2001**, *74*, 419.

16. Marosi, G.; Márton, A.; Anna, P.; Bertalan, G.; Marosfoi, B.; Szép, A. *Polym. Degrad. Stabil.* **2002**, *77*, 259.

17. Estevāo, L. R. M.; Le, B. M.; Delobel, R.; Nascimento, R. S. V. *Polym. Degrad. Stabil.* **2005**, *88*, 444.

18. Gallo, E.; Schartel, B.; Acierno, D.; Russo, P. *Eur. Polym. J.* **2011**, *47*, 1390.

19. Laoutid, F.; Ferry, L.; Lopez-Cuesta, A. *Polym. Degrad. Stabil.* **2003**, *82*, 357.

20. Li, N.; Xia, Y.; Mao, Z. W.; Wang, L. *Polym. Degrad. Stabil.* **2012**, *97*, 1737.

21. Levichik, S. V.; Levchik, G. F.; Camino, G.; Coata, L. *Fire Mater.* **1996**, *20*, 183.

22. Lewin, M.; Endo, M. *Polym. Adv. Technol.* **2003**, *14*, 3.

23. Wu, K.; Wang, Z. Z.; Hu, Y. *Polym. Adv. Technol.* **2008**, *19*, 1118.

24. Luo, J. Y. The Use of Ammonium Polyphosphate; Chemical Industry Press: Beijing, **2006**; Vol. *16*, p 1.

25. Hsu, J.; Choi, K. Y. *J. Appl. Polym. Sci.* **1987**, *33*, 329.

26. Vassiliades, A. E. Formation of Microcapsules by Interfacial Cross-Linking of Emulsifier, and Resulting Microcapsules. US Patent 3,875,074, **1972**.

27. Michel, B.; Bourbigot, S.; Le, B. M.; Delobel, R. *Polym. Int.* **1999**, *48*, 264.

28. Xie, R. C.; Qu, B. *J. Polym. Degrad. Stabil.* **2001**, *71*, 395.

29. Hu, X. P.; Li, Y. L.; Wang, Y. Z. *Macromol. Mater. Eng.* **2004**, *289*, 208.

30. Kranes, A.; Lange, A.; Ezrin, M. Plastics Analysis Guide; Hanser Publishers: New York, **1983**.